Developmental Biology **219,** 224–236 (2000)
doi:10.1006/dbio.2000.9612, available online at http://www.idealibrary.com on IDEAL®

Influence of FGF4 on Digit Morphogenesis during Limb Development in the Mouse

Valerie Ngo-Muller[1] and Ken Muneoka[2]

Department of Cell and Molecular Biology, Tulane University, New Orleans, Louisiana 70118

Much of what we currently know about digit morphogenesis during limb development is deduced from embryonic studies in the chick. In this study, we used *ex utero* surgical procedures to study digit morphogenesis during mouse embryogenesis. Our studies reveal some similarities; however, we have found considerable differences in how the chick and the mouse autopods respond to experimentation. First, we are not able to induce ectopic digit formation from interdigital cells as a result of wounding or TGFβ-1 application in the mouse, in contrast to what is observed in the chick. Second, FGF4, which inhibits the formation of ectopic digits in the chick, induces a digit bifurcation response in the mouse. We demonstrate with cell marking studies that this bifurcation response results from a reorganization of the prechondrogenic tip of the digit rudiment. The FGF4 effect on digit morphogenesis correlates with changes in the expression of a number of genes, including *Msx1, Igf2,* and the posterior members of the *HoxD* cluster. In addition, the bifurcation response is digit-specific, being restricted to digit IV. We propose that FGF4 is an endogenous signal essential for skeletal branching morphogenesis in the mouse. This work stresses the existence of major differences between the chick and the mouse in how digit morphogenesis is regulated and is thus consistent with the view that vertebrate digit evolution is a relatively recent event. Finally, we discuss the relationship between the digit IV bifurcation restriction and the placement of the metapterygial axis in the evolution of the tetrapod limb.

Key Words: **FGF4; limb development; digit development; cell migration; limb evolution; mouse.**

INTRODUCTION

The vertebrate limb is a classic model system used for studying morphogenesis and, in particular, cell communication responsible for skeletal pattern formation. Elements of the vertebrate limb skeleton originate in mesenchymal condensations, which arise following epithelial–mesenchymal interactions. Such interactions include reciprocal signaling between a specialized epithelium located at the distal tip of the early limb bud, the apical ectodermal ridge (AER), and the underlying mesenchyme, called the progress zone (reviewed in Johnson and Tabin, 1997). The AER stimulates limb outgrowth by maintaining the progress zone cells in a highly proliferative and undifferentiated state. Because of distal outgrowth, the mesenchymal cells on the proximal margin of the progress zone are no longer under the influence of the AER, and some of them aggregate to form condensations. These condensations later differentiate into cartilage that forms a prepattern for the bony skeleton. While skeletal pattern specification occurs in the progress zone, the limb skeleton itself forms in a proximal to distal sequence by a series of branching and segmentation events that are spatially and temporally controlled (Shubin and Alberch, 1986).

In the early bud, before any condensation has occurred, three interdependent signaling centers essential to outgrowth and patterning in the three cardinal axes are being established (reviewed in Johnson and Tabin, 1997). Anterior–posterior patterning is mediated by the zone of polarizing activity (ZPA), a small block of mesodermal tissue near the posterior junction of the limb and the body wall. Factors mediating ZPA activity include members of the *HoxD* family, which are homeobox transcription factors, and secreted molecules like Sonic hedgehog (SHH) and the bone morphogenetic proteins (BMP) BMP2 and BMP4. Proximal–distal limb outgrowth is controlled by the AER that expresses members of the fibroblast growth factor (FGF) family, including FGF2, 4, and 8 (Savage *et al.*, 1993;

[1] Current address: INSERM U129, ICGM Cochin Port-Royal, 24, Rue du Fbg St Jacques, 75014 Paris, France.

[2] To whom correspondence should be addressed at the Department of Cell and Molecular Biology, Tulane University, New Orleans, LA 70118. Fax: (504) 865-6785. E-mail: kmuneoka@mailhost.tcs.tulane.edu.

0012-1606/00 $35.00

Fallon *et al.,* 1994; Niswander and Martin, 1992; Niswander *et al.,* 1993; Vogel *et al.,* 1996; Crossley *et al.,* 1996). *Fgf2* and *Fgf8* are expressed throughout the AER, while *Fgf4* expression is restricted to the posterior AER. FGFs are expressed in the AER before the primary prechondrogenic condensation begins to form [mouse embryonic day 10 (E10)] and continue to be expressed until the last condensations of the autopod appear (mouse E12), at which time the AER becomes morphologically undetectable. At present, experimental evidence indicates that these FGFs are responsible for the signaling between the AER and the progress zone.

The concept of the progress zone was defined by Wolpert and his colleagues (Summerbell *et al.,* 1973) as a labile population of cells in which positional identities become fixed at the time they leave the zone. According to the current model, the genes expressed in this region reflect the integration of axial patterning information, and they thus prefigure the chondrogenic aggregation events of the forming skeleton. In the advanced limb bud, when the autopod founder cells start to aggregate, the ZPA and the AER are regressing, suggesting that patterning events that specify both the anterior–posterior and the proximal–distal axes are complete. Many genes are expressed in the progress zone at that time, including members of the *HoxD* cluster, which are detected as nested patterns centered on the ZPA, and have been proposed to encode positional information (Dollé *et al.,* 1989). This hypothesis is supported by a substantial body of data, including those of Yokouchi *et al.* (1991), which show that when the expression domains of *HoxA* and *HoxD* genes are superimposed, the cartilage elements in the chick limb are prefigured. In recent years, several *Hox* gene disruption and targeted misexpression analyses have been performed in the mouse, revealing a complex network of genetic interactions between paralogous and nonparalogous *Hox* genes (reviewed in Rijli and Chambon, 1997). Experimental data suggest that *HoxA* and *HoxD* genes are involved in regulating cell adhesion properties affecting the branching and segmentation pattern of chondrogenic condensations, as well as their growth rates (Yokouchi *et al.,* 1995; Goff and Tabin, 1997). Though a number of genes involved in limb patterning have been identified, the molecular signals that control mesenchymal cell condensation and cartilage patterning are still largely unknown.

Mesenchymal condensations are initiated as changes occur in the extracellular matrix, bringing cells in closer proximity. Condensations grow by recruitment of mesenchymal cells at the distal end of the developing limb. Mesenchymal cells that do not form aggregates remain loosely packed and become interdigital cells, eventually undergoing apoptosis, a process that participates in the shaping of the autopod by separating the digits. Interdigital cells remain undifferentiated and express *Msx* genes before entering the cell death pathway, while cells that form mesenchymal condensations cease to express *Msx* genes. There is considerable evidence obtained from studies on the chick limb indicating that the specification of these two cell fates is mediated by the BMPs (Macias *et al.,* 1996; Yokouchi *et al.,* 1996; Zou and Niswander, 1996; Zou *et al.,* 1997; Merino *et al.,* 1998). In addition, interdigital cells respond to ectodermal wounding or to TGFβ bead implantation by forming ectopic digits (see Gañan *et al.,* 1996). In this context, local administration of FGFs prevents ectopic chondrogenesis by interdigital cells. In the current view of limb and digit morphogenesis, FGFs are thought to play a role in maintaining progress zone cells in a proliferative and undifferentiated state and antagonizing the effects of BMPs and TGFβs. In addition, recent reports indicate that FGF2 and FGF4 influence cell movements in both the chick bud (Itoh *et al.,* 1996; Li *et al.,* 1996; Kostakopoulou *et al.,* 1997; Li and Muneoka, 1999) and the mouse bud (Webb *et al.,* 1997).

In this study we used an *in vivo* experimental approach in order to investigate the role of FGF4 in the formation of the mouse limb skeletal pattern during digit formation stages. We employed the *ex utero* surgical technique (see Ngo-Muller and Muneoka, 1999), which allowed us to manipulate mouse embryos and permitted them to further develop *in vivo,* in order to study digit morphogenesis. We first assessed whether mouse interdigital mesenchyme had the potential to form extra digits under the conditions previously used in the chick. We found that ectodermal wounding or application of a TGFβ1 bead never elicited the formation of ectopic cartilage. In contrast, FGF4 bead implantation resulted in a proximal inhibition of cartilage differentiation, which correlated with a change in the expression pattern of a number of genes, including *Msx1, Igf2,* and the posterior members of the *HoxD* cluster. In addition, FGF4 induced a distal bifurcation that was restricted to digit IV, a response not reported from similar experiments in the chick. Thus, there appear to be important differences in interdigital cell plasticity between chick and mouse limbs. The digit IV bifurcation response involved a reorganization of distal prechondrogenic cells to form two digit tips and this occurred without altering cell proliferation or apoptosis in the responsive cells. Our evidence indicates that FGF4 is an endogenous signal essential for skeletal branching morphogenesis in the mouse. Finally, we discuss the relationship between the digit IV bifurcation restriction and the distal path of the proposed primitive metapterygial axis from which skeletal branching morphogenesis evolved among tetrapod vertebrates.

MATERIALS AND METHODS

Bead Preparation

Human recombinant FGF4 or porcine TGFβ1 (R&D Systems) was applied to the mouse left hindlimb bud using agarose beads. Affi-Gel Blue beads (150–200 μm; Bio-Rad) were selected and washed in phosphate-buffered saline (PBS). Twenty beads were incubated in a 2-μl drop of FGF4 (500 μg/ml) or TGFβ1 (50 μg/ml)

for at least 1 h at 4°C. Control beads were incubated in PBS 0.1% BSA under the same conditions.

Mouse Embryo Manipulations

Bead implantation, ectoderm wounding, and DiI injections in the developing mouse limb bud were performed using the *ex utero* surgical technique previously described (Ngo-Muller and Muneoka, 1999). Briefly, timed-pregnant CD1 mice (Harlan Sprague–Dawley) were selected at E12.5 or E13.5 (Wanek *et al.*, 1989) and anesthetized using sodium pentobarbital (0.06 mg/g body weight) and droperidol/fentanyl (80 and 1.6 μg/animal). The abdominal cavity was opened, and embryos were released from the uterus by making an incision along the avascular side of the uterine wall. Embryos were submerged in lactated Ringer's solution, positioned, and stabilized using cotton balls. Extraembryonic membranes were cut to expose the left hindlimb.

Affi-Gel Blue beads were pinned onto a sharpened tungsten needle, and a graft site was created using another sharpened needle to "tunnel" through the tissue to the implantation site. The pinned bead was then inserted into the tunnel and released at the graft site. Beads were implanted in the distal mesenchyme, just under the marginal vein that runs underneath the distal ectoderm. Ectoderm wounding [T-cut; see Hinchliffe and Horder (1993)] or removal of interdigital marginal ectoderm was performed using a sharpened tungsten needle. Injection of DiI (1,1-dioctadecyl-3,3,3′,3′-tetramethylindocarbocyanine perchlorate; 0.1 μg/μl in 0.3 M sucrose, 1% ethanol, and 0.05% Nile blue sulfate, CellTracker; Molecular Probes) was performed using pulled glass micropipettes and a microinjector.

Following manipulations, the extraembryonic membranes and the abdominal wall were sutured. Fetuses were allowed to develop from 12 h to 6 days following surgery, at which time they were processed for whole-mount skeletal staining, *in situ* hybridization, cell proliferation, or cell migration studies.

Skeletal Staining

Skinned and eviscerated E18.5 embryos were fixed in Bouin's fixative and stained with Victoria blue (Bryant and Iten, 1974) to observe the chondrogenic pattern. Limbs were cleared in methyl salicylate. In earlier stages at which Victoria blue is not suitable to stain cartilage (E13–E14.5), Alcian blue staining of sulfated and nonsulfated proteoglycans was performed on paraffin sections as described in Humason (1972).

Proliferating Cell Nuclear Antigen (PCNA) Immunodetection

Embryos were fixed in methacarn in order to preserve the immunoreactivity of the PCNA form that is associated with DNA synthesis and processed for immunodetection with PC10 mouse monoclonal antibody (Santa Cruz Biotechnology, Santa Cruz, CA) according to the manufacturer's protocol. Briefly, samples were dehydrated, paraffin-embedded, and sectioned at 7 μm. Sections were rehydrated, preblocked in 10% sheep serum, incubated with PC10 antibody (diluted 1:200 in 2% sheep serum in PBS), incubated with secondary sheep antibody anti-mouse IgG (whole molecule) conjugated to FITC (Sigma) (diluted 1:50 in 2% sheep serum in PBS), and mounted with anti-fading agent (Vectashield; Vector). Fluorescent signal was viewed using a fluorescence microscope (Olympus) with the appropriate filter.

TUNEL Staining

Apoptotic cells were labeled by the TdT terminal transferase dUTP–biotin nick end labeling (TUNEL) method, following the instructions of the manufacturer (Apoptag kit; Oncor). Briefly, paraformaldehyde-fixed embryos were dehydrated, paraffin-embedded, sectioned at 7 μm, rehydrated, and processed for apoptosis detection by staining with DAB. Sections were counterstained with methyl green.

RNA Probes

Murine antisense RNA *in situ* probes were prepared as described: *Fgf8* [cloned in pCRII vector (Invitrogen) by RT-PCR using primers described in Ghosh *et al.* (1996)]; *Gli* (Walterhouse *et al.*, 1993); *HoxD11*, *HoxD12*, and *HoxD13* (Dollé *et al.*, 1989); *Igf2* (van Kleffens *et al.*, 1998); *Msx1* and *Msx2* (Bell *et al.*, 1993; Brown *et al.*, 1993); and *Syn1* (Vihinen *et al.*, 1993). Digoxigenin (DIG) labeling was performed according to the manufacturer's protocol (RNA DIG-labeling kit; Boehringer Mannheim).

In Situ Hybridization

Limbs processed for *in situ* hybridization were washed in PBS and fixed in 4% paraformaldehyde 0.1% Tween-20 in PBS (pH 7.2) overnight. Samples were dehydrated in a graded ethanol series, embedded in paraffin, and serially sectioned at 7 μm. *In situ* hybridization was carried out according to the following protocol, adapted from Wilkinson and Nieto (1993). Slides were deparaffinized and rehydrated in a graded ethanol series. Samples were digested with proteinase K, acetylated in 0.1 M triethanolamine, and dehydrated in a graded ethanol series. DIG-labeled RNA probe was denatured for 15 min at 75°C, applied to the dry sections, and incubated at 60°C overnight. Samples were washed in 5× SSC at 60°C and 50% formamide/2× SSC at 45°C and then digested with 20 μg/ml RNase A and 5 U/ml RNase T1. Slides were washed in 2× SSC at 37°C, 0.1× SSC at 45°C, and 0.1× SSC at room temperature (RT). Slides were incubated with preabsorbed anti-DIG antibody and incubated in a humidified chamber at 4°C overnight. Slides were developed using BM purple (Boehringer Mannheim) at 4°C or at RT for 1–48 h. Sections were counterstained with safranin O (0.2% w/v in 1% glacial acetic acid), dehydrated in a graded ethanol series, cleared, and mounted with Permount. *In situ* hybridization analyses were performed on representative serial sections from two to four limbs hybridized individually for each gene.

RESULTS

Procedures Causing Extra Digits in the Chick Are Not Effective in the Mouse

In an attempt to study cartilage morphogenesis in the mouse limb bud, we first tried to induce ectopic interdigital cartilage formation in the mouse using procedures known to induce ectopic chondrogenesis in the chick. These procedures were performed on Hamburger and Hamilton (1951) stage 28–29 chick leg bud. At these stages, four digit condensations are apparent, and the webbing between all digits is pronounced. The manipulations include removing the marginal ectoderm and underlying mesoderm or applying a T-cut to the dorsal aspect of the third interdigit of the

leg bud (Hurle *et al.*, 1989; Hinchliffe and Horder, 1993). Implantation of beads soaked with recombinant TGFβ1 (50 μg/ml) in the distal part of the third interdigit also induces ectopic cartilage (Gañan *et al.*, 1996).

E12.5 mouse hindlimb buds, which are equivalent to stage 28–29 chick leg buds (Wanek *et al.*, 1989), were manipulated using *ex utero* surgery. The marginal ectoderm and underlying mesoderm of the interdigit III–IV were removed (five limbs), or a T-cut was applied to the dorsal interdigit III–IV ectoderm (eight limbs). In another set of experiments, Affi-Gel Blue beads loaded with recombinant TGFβ1 (50 μg/ml) were implanted at the distal tip of the interdigit III–IV (seven limbs). Manipulated mouse fetuses continued to develop *ex utero* for 2 to 6 days, after which they were processed for whole-mount skeletal analyses. None of the manipulations induced interdigital ectopic chondrogenesis (20 cases total, not shown). Ectoderm wounding did not elicit any morphological alteration of the limb skeleton, while TGFβ1 locally inhibited chondrogenesis (not shown). In the chick, these manipulations are thought to redirect interdigital cell commitment toward the chondrogenic pathway and demonstrate that interdigital tissue shows a high degree of plasticity. Thus, unlike in the chick, mouse interdigital cells were not able to undergo chondrogenic differentiation under these experimental conditions. Our results indicate the existence of fundamental differences in plasticity between mouse and chick interdigital tissue.

FGF4-Induced Skeletal Abnormalities

Since FGF4 plays an important role in early limb development, we tested whether FGF4 signaling may regulate cartilage morphogenesis later in development. Affi-Gel Blue beads soaked in PBS with 0.1% BSA or loaded with human recombinant FGF4 (500 μg/ml) were implanted in the distal mesenchyme of E12.5 mouse hindlimb buds. Beads were placed either at the distal tip of the forming digit (digit III or IV) or at the second or third interdigital region (interdigit II–III or III–IV). Fetuses were collected 12 h to 6 days after operation, and stage-appropriate limbs were stained with Victoria blue to reveal the condensing limb skeleton. Implantation of a control bead had no effect on the morphology of the limb (Fig. 1A). In contrast, FGF4 bead implantation induced several morphological alterations of the limb connective tissue and skeleton. First, FGF4 application in E12.5 mouse limb buds induced temporary webbing. Forty-eight hours after the operation, when digit separation is almost complete in contralateral limbs, operated limbs systematically showed webbing in the interdigit where the bead had been implanted (not shown). This syndactyly feature was temporary and could not be observed 6 days after operation on whole-mount preparations. However, potential syndactyly could have been masked by the fact that mouse digits undergo a secondary fusion at E17 (Maconnachie, 1979). We thus carried out a histological analysis of FGF4 implanted limbs and confirmed that digits III and IV were well separated (Fig. 1F). Histological sections also revealed that the FGF4 bead had no effect on digit separation but did have a local inhibitory effect on the formation of the ventral tendon of digit adjacent to the bead (Fig. 1E).

Second, the operated limbs showed a significant reduction in the diameter and length of the skeletal elements adjacent to the bead. The effect was quantified by comparing measurements of the length of equivalent skeletal elements from implanted and contralateral sides of the same embryo. Although individual embryos were affected to differing extents, shortening of the autopod cartilage elements was observed in >90% of the cases (n = 20). Differences in the length of the cartilage elements were first detectable at E14.5. Differences in size became more apparent on subsequent days such that by E18.5 the implanted limbs averaged 84 ± 5% (SEM) (n = 20) of the length of the contralateral control elements when the length of metatarsal and phalanges were considered together.

In addition to the shortening of the limb skeleton, other cartilage phenotypes were observed. When limbs were collected 12 h after operation and stained with Alcian blue, we observed a total absence of staining of digits III and IV cartilaginous condensations from the level of the bead to the distal tip (not shown). In addition, the morphology of the metatarsal skeletal elements adjacent to the bead was altered. Analysis revealed a noticeable reduction in the width of metatarsal elements in 55% of the cases (n = 20, Figs. 1B and 1E). For instance, absence of ossification was frequently observed. The ossification center is normally visualized in contralateral control limbs as a discontinuity of Victoria blue staining in the middle of a skeletal element (Fig. 1A, arrow). In 90% of the limbs receiving FGF4 beads, this discontinuity was not observed in metatarsal and phalanges located close to the bead (n = 20, Fig. 1B, arrow).

Finally, a striking effect of FGF4 application was the induction of a branching of the terminal phalanges P2 and P3, or P3 only, in 50% of the cases (n = 20, Figs. 1C and 1D). The bifurcation systematically occurred on digit IV, and the additional skeletal element was always branched to an existing element and never appeared as ectopic cartilage (i.e., not connected to existing skeletal elements). The FGF4-induced bifurcations always formed a mirror-symmetric pattern of distal skeletal elements. The digit IV bifurcation was observed regardless of whether the bead was placed at the tip of digit III or IV or in the interdigit III–IV, but never when the bead was placed in the interdigit II–III. Thus FGF4 can influence digit formation at a distance equal to the interdigital regions between digits III and IV. In our data set we find a total of 31 opportunities where digit II (n = 9) or digit III (n = 22) was exposed to FGF4 levels high enough to induce digit bifurcation, yet we find that in no case did we observe a bifurcation response. On the other hand, our data indicate that of 18 exposures to FGF4, we observe bifurcation of digit IV in 10 cases (56%). Our results indicate that of the three central digits tested there is an absolute restriction of the FGF4-induced bifurcation to digit IV. Similar studies on stage 9 (E13.5) limbs resulted in no

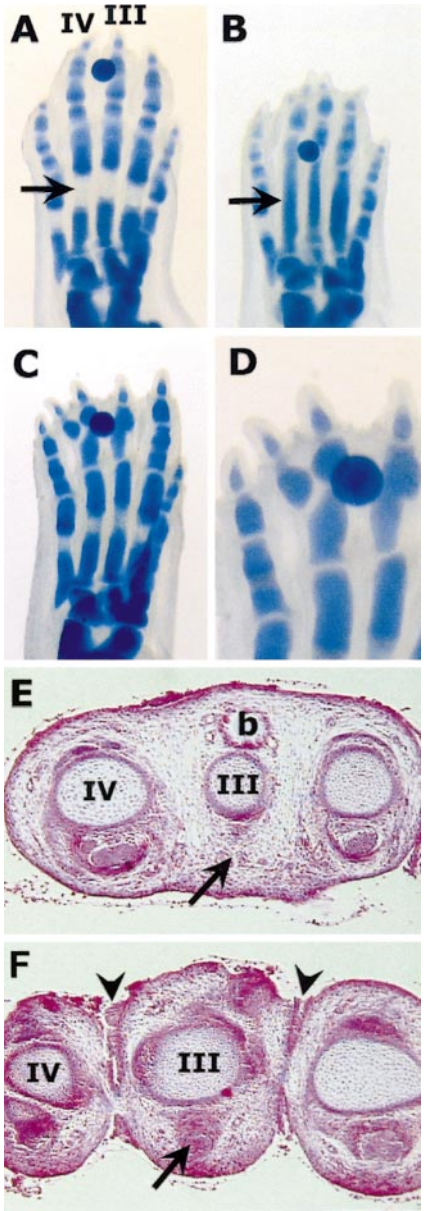

FIG. 1. FGF4 bead implantation in E12.5 mouse left hindlimb bud causes inhibition of cartilage growth and differentiation as well as connective tissue alteration. All limbs were collected at E18.5. Digits are numbered in Roman numerals. Whole-mount Victoria blue staining of limbs following FGF4 bead implantation in the distal interdigital mesenchyme (B, C, D) or control bead (A). (A, B, C, and D) Limbs are shown from a dorsal view, with anterior on the right and distal toward the top. Staining reveals cartilaginous elements; arrow in A points to the ossification center of a metatarsal element and arrow in B points to the expected position of this ossification center, which is not detectable in the operated limb in B. (D) Magnification of digits IV and V in (C). (E and F) Following analysis with Victoria blue staining, some FGF4-implanted limbs were paraffin-embedded, cross-sectioned, and stained with Mallory's in order to assess whether digit separation had occurred. Anterior is to the right, and dorsal is toward the top. (E) Cross section illustrates the reduced diameter of digit III as well as the absence of digit III tendon (arrow). b. bead. (F) A more distal cross section illustrates complete digit separation (arrowheads). Arrow points at digit III tendon, which is present at this level (compare with E).

effect on skeletal morphology (not shown, 11 cases), thus indicating that the effect of FGF4 on digit bifurcation and chondrogenesis was stage-specific.

Most of these observations differed from those reported in the chick, in which FGF4 bead implantation into the interdigital tissue of the leg bud was reported to cause the formation of webbed digits and to induce a delay in chondrogenesis (Macias *et al.*, 1996; Buckland *et al.*, 1998; Merino *et al.*, 1998). The syndactyly observed in the chick results from a stimulation of interdigital cell proliferation and an inhibition of interdigital cell apoptosis (Macias *et al.*, 1996). In the mouse, we observed a delay in digit separation; however, digit separation appeared normal at birth. More importantly, FGF4 was able to elicit a variety of morphological alterations of the cartilage. Thus, our results indicate that mouse and chick limb buds respond differently to FGF4 application. The induction of cartilage branching in the mouse limb bud by FGF4 led us to investigate (1) the origin of the cells contributing to the bifurcation, (2) cell proliferation associated with the FGF4 bead, and (3) FGF4 influence on apoptosis.

FGF4 Does Not Modify Cell Proliferation in Interdigital Cells

FGF4 is known to be mitogenic for early mouse limb bud cells *in vitro* (Niswander and Martin, 1992) and for interdigital cells of the chick limb *in vivo* (Macias *et al.*, 1996). In our studies, we assayed cell proliferation *in vivo* by detecting PCNA, which is expressed in cells from late G1 through the S phase of the cell cycle, using immunocytochemistry. Embryos were collected 24 h after operation and processed for immunodetection with PC10 antibody. PCNA immunodetection on normal limbs showed that interdigital regions stained negative for PCNA, as expected. In the presence of a control bead in the interdigit III–IV, labeled cells could be seen around the bead (not shown), indicating a growth response associated with the microsurgical procedure. When an FGF4 bead was implanted, a level of PCNA labeling in the interdigital cells similar to that in the control was observed ($n = 4$, Fig. 2A). In addition, no difference in PCNA staining could be observed within the cartilage-forming regions. These results indicate that the FGF4 bead does not influence proliferation of chondrogenic or interdigital tissues.

FGF4 Transiently Affects Apoptosis in Interdigital Cells

Apoptosis was assessed using the TUNEL method on embryos collected 12 or 24 h after operation. At E13.0–

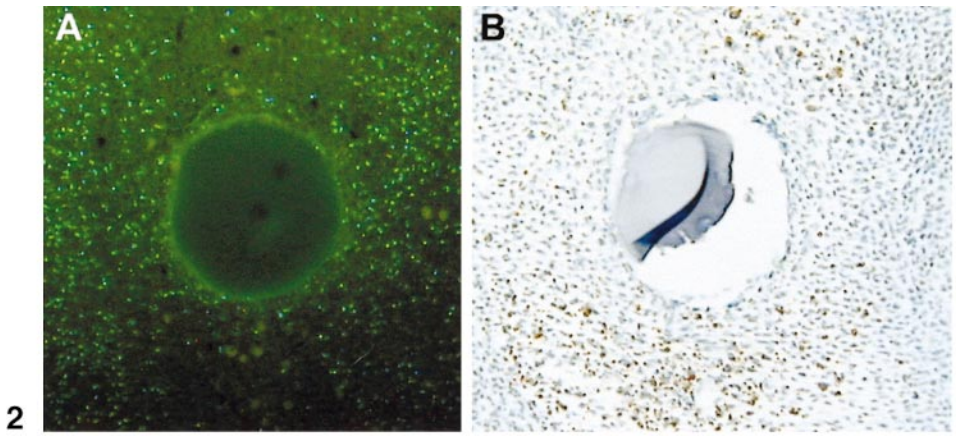

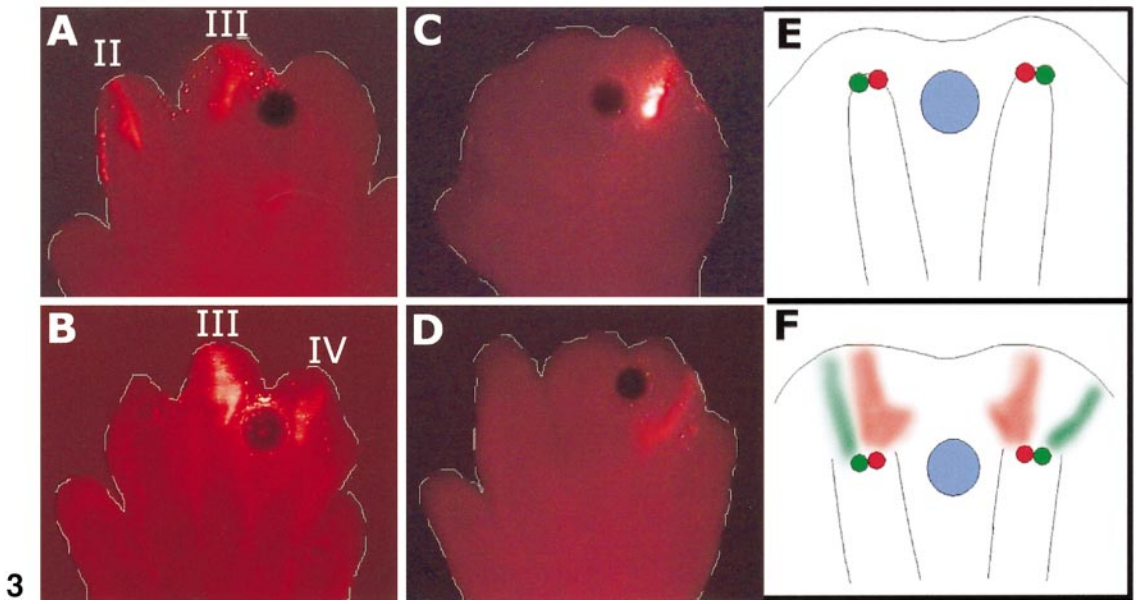

FIG. 2. Pattern of cell proliferation and apoptosis in interdigit III–IV of FGF4-implanted limbs collected after 24 h. Ventral view of horizontal sections, with posterior to the right and distal to the top. (A) Cell proliferation was assessed by proliferating cell nuclear antigen staining using monoclonal PC10 primary antibody and an FITC-conjugated secondary antibody. Levels of PCNA staining with an FGF4 bead are similar to those observed with a control bead (not shown). (B) Apoptosis was assessed using TUNEL, which stains apoptotic cells brown. Sections were counterstained with methyl green. Apoptotic cells are visible around the bead in interdigit III–IV, comparable to what was observed in a control interdigit (not shown).

FIG. 3. FGF4 influences prechondrogenic cell movement. Cells located at the distal tip of prechondrogenic regions were labeled with DiI, and an FGF4 bead was simultaneously implanted in the interdigit III–IV. Ventral view of whole-mount preparation cleared in sucrose and viewed under low magnification fluorescence microscopy. Anterior is to the left, and distal is toward the top. Digits are numbered in Roman numerals. The contour of each limb is outlined with a white pencil line. Manipulated limbs were collected after 48 (A, C) and 72 h (B, D). (E) A map of DiI injection sites: red dots represent the locations of posterior digit III and anterior digit IV injection sites, and green dots represent the locations of anterior digit III and posterior digit IV injection sites. The bead is represented by a blue disc. (A) During normal outgrowth, DiI-injected cells at the tip of digit II form a trail after 48 h. The trail expands away from the injection site in a distal direction. Following implantation of an FGF4 bead in the interdigit III–IV next to a posterior DiI-labeled site at the distal tip of digit III, labeled cells first expand toward the bead and then in a distal direction. (B) Posterior and anterior injections were performed on digit tips III and IV, respectively. A bifurcation of digit tip IV was observed, and DiI-labeled cells participated in the branching that expanded toward the FGF4 bead. (C) A posterior injection was performed on digit tip IV. Labeled cells formed a trail expanding away from the injection site in a distal direction. (D) A posterior injection was performed on digit tip IV, and a bifurcation of digit IV was observed. DiI-labeled cells formed a trail along the branching expanding away from the FGF4 bead. (F) A fate map resulting from the analysis of 12 limb buds that had received anterior or posterior DiI injections. Red trails indicate the fate map of injected prechondrogenic cells located close to the bead and green trails of injected prechondrogenic cells located farthest away.

E13.5, apoptosis is normally observed in the interdigital regions as well as in the distal ectoderm and the underlying mesenchyme, in both the mouse and the chick (reviewed in Chen and Xhao, 1998). Twelve hours after FGF4 bead implantation in mouse limb buds (E13.0), apoptotic cells could not be detected in the interdigit where the bead had been implanted (not shown), thus indicating that the onset of apoptosis is inhibited by FGF4 application. When embryos were collected 24 h after the operation (E13.5), labeled apoptotic cells could be seen associated with the bead, similar to where apoptosis normally occurs at that stage (Fig. 2B). Our results indicate that FGF4 inhibits the onset of interdigital cell apoptosis in the mouse, and these observations are comparable to those obtained in the chick.

FGF4 Influences Outgrowth of Prechondrogenic Cells

The results gathered on cell proliferation and apoptosis suggested that the cells involved in cartilage branching were not of interdigital origin, but were derived from cells in the digit ray. To test this hypothesis, we carried out studies to fate map the FGF4 response using DiI cell marking in conjunction with FGF4 bead implantation. We performed simultaneous implantation of an FGF4 bead in the interdigit III–IV and microinjection of the lipophilic dye DiI in the prechondrogenic region at the distal tip of digits II, III, and IV. Embryos were collected 48 and 72 h after operation, 48 h being the minimal amount of time after which a bifurcation could be morphologically detected. After 48 h, a control injection made at the tip of digit II showed a continuous line of labeled cells from the injection site to the distal tip of the digit, perfectly parallel to the proximal–distal axis (Fig. 3A). We then injected DiI at the tip of digit IV (bifurcation frequency of 56%) or at the tip of digit III (bifurcation frequency of 0%). For digits III and IV, injections were administered in two different regions separating the digit tip into an anterior half and a posterior half. For digit III the anterior half represents the region farthest away from the bead and the posterior half the region closest to the bead. For digit IV the situation is reversed with the anterior half closest to the bead and the posterior half farther away from the bead (see Fig. 3E). Each injection site was mapped by videotaping each operation.

In the first group of experiments, the injection was made in the posterior of digit tip III and the anterior of digit IV, i.e., into regions of each digit closest to the FGF4 bead (Figs. 3A and 3B; see Fig. 3E). The behavior of cells in both digits III and IV was similar and a symmetrical pattern of DiI labeling was observed. Labeled cells were found along a line going from the injection site to the distal ectoderm and in both cases there was an initial deflection of labeled cells directed toward the bead ($n = 6$; Fig. 3C). Labeled cells could be identified as cartilage cells by examining the limbs after sectioning and clearing in sucrose (not shown). The trail of DiI-labeled cells was never in direct contact with the bead. Some isolated cells were seen close to the bead and were most likely macrophages, identifiable by a bright vesicular DiI staining. After 48 h, the trail of labeled cells could be seen directed toward the bead, while after 72 h, the subsequent trail was curving back toward the distal ectoderm (Figs. 3A and 3B). When a bifurcation was observed, labeled cells contributed to the branch closest to the bead, and no labeled cells contributed to the symmetric branch located away from the bead (Fig. 3B).

In a second study, regions located farthest away from the FGF4 bead was targeted, i.e., the posterior half of digit IV and the anterior half of digit III (Fig. 3E). As in the previous study the behavior of cells in digits III and IV with respect to FGF4 was similar, although there were dramatic differences in their developmental fate. The fate map of the anterior half of digit III indicates that cells display no apparent response to FGF4. We observe a trail of labeled cells that extends from the injection site to the tip of the digit (not shown). This pattern of labeling is identical to that observed in control experiments in the absence of FGF4 (see Fig. 3A) and indicates that these cells are unaffected by FGF4. DiI labeling of the posterior half of digit IV indicates that this cell population also behaves in a manner that is identical to that in control studies, i.e., DiI-labeled cells formed a straight trail that extended from the injection site to the tip of the digit (Fig. 3D). However, in this case these cells participated in the formation of a bifurcated digit tip that angled away from the proximal–distal axis of the limb. Thus, while the behavior of these cells was normal, the direction of their migration path was significantly modified. These data suggest that digit tip cells respond to an apical signal that defines the distal boundary of each digit and that ectopic FGF4 induces a duplication of the digit IV distal boundary. Thus, the bifurcation response results from prechondrogenic digit tip cells responding to two distal boundaries. In summary, we find that the bifurcation response results from the bisection of a prechondrogenic cell population at the distal tip of digit IV. Cells closest to the bead display an initial deflection toward the FGF4 bead then migrate toward one (anterior) of the bifurcated digit tips (see Fig. 3F). The prechondrogenic cells farthest away from the FGF4 bead appear unaffected, but migrate toward the digit tip of the symmetric branch of the bifurcation. Interestingly, the prechondrogenic cells of digit III display a similar behavior yet we never observe a digit III bifurcation response.

FGF4 Affects Msx1, HoxDs, and Igf2 Gene Expression

To better understand the FGF4-induced morphogenetic changes, including growth inhibition and formation of branching, we investigated gene expression in the tissue surrounding the bead implanted distally in interdigit III–IV. Gene expression was analyzed by section *in situ* hybridization of limbs collected 24, 48, or 72 h after operation. In order to describe FGF4 effects on gene expression, we considered three subpopulations of cells, the interdigital cells located in interdigit III–IV (around the bead), the prechondrogenic cells located at the distal tip of digits III

and IV, and the chondrogenic cells of digit rays III and IV. We analyzed the expression of several genes that have been implicated in digit morphogenesis, including the *Msx* genes, *Fgf8*, *Gli*, *Syn1*, *Igf2*, and the posterior *HoxD* genes. The expression of *Msx2*, *Fgf8*, and *Gli* was not modified 24 or 48 h after FGF4 bead implantation (not shown). The normal interdigital expression of *Syn1* was transiently down-regulated 24 h after bead implantation, and after 72 h *Syn-1* expression returned to normal (not shown).

Msx1 expression was markedly altered 24 and 48 h after FGF4 bead implantation. During the stages studied (E12.5 to E14.5), *Msx1* expression is restricted to interdigital cells and to prechondrogenic cells at the digit tip (Reginelli *et al.*, 1995; Figs. 4A and 4B). In operated limbs collected after 24 h (E13.5), *Msx1* expression in interdigital cells was affected in a stage-dependent manner. In early stage 12.5 limb buds, *Msx1* expression was down-regulated (Fig. 4C), whereas *Msx1* expression was up-regulated in late stage E12.5 buds (Fig. 4D). FGF4 had a stage-independent effect on *Msx1* expression in prechondrogenic and chondrogenic cells of the digit ray. Prechondrogenic cells were not affected by FGF4, while Msx1 expression was up-regulated in chondrogenic cells (Figs. 4C and 4D). Of note, the width of chondrogenic rays (visualized as *Msx1*-negative chondrogenic cells) was markedly reduced at the level of the bead (compare Figs. 4C and 4D to 4B). After 48 h, *Msx1* expression was detected in prechondrogenic cells and in interdigit III–IV that had not regressed (Fig. 4M). *Msx1* expression was largely absent in chondrogenic cells at this stage. The shape of the digit rudiment, based on the *Msx1*-negative staining, was irregularly reduced at the level of the FGF4 bead and enlarged at the distal tip (Fig. 4M).

FGF4 had an opposite effect on *Igf2* gene expression. During the stages studied (E12.5 and E14.5), *Igf2* expression in the autopod is largely complementary to Msx1 expression, its domain is restricted to chondrogenic areas and is absence in prechondrogenic and interdigital cells (van Kleffens *et al.*, 1998; Figs. 4E, 4F, and 4H). In FGF4 bead-implanted limbs collected 24 h after operation (E13.5), *Igf2* expression locally down-regulated in digit rays III and IV (Fig. 4G, $n = 2$). In operated limbs collected at E14.5, *Igf2* expression pattern was altered by FGF4 at the digit tip. The distal tip of the digit ray normally displays a tapered expression of *Igf2* associated with skeletal formation (Fig. 4H); however, in FGF4-treated digits the distal *Igf2* expression domain was rounded and wider than controls (Fig. 4I, arrow). FGF4 also influenced the interruption of *Igf2* expression that is normally observed at forming joints (compare Fig. 4F to 4G and 4H to 4I) and caused a reduction in the width of *Igf2* staining proximally at the level of the bead (compare Fig. 4H to 4I). In general, the FGF4-induced expression domains of *Msx1* and *Igf2* were complementary (compare Figs. 4I and 4M).

HoxD11, *HoxD12*, and *HoxD13* gene expression patterns were affected in chondrogenic cells in a manner similar to what was observed with *Igf2*, i.e., delayed progression of expression pattern (Figs. 4J–4L). Altogether the pattern of *HoxD* gene expression seemed to be retarded in that it seemed to retain the characteristics of the expression pattern observed at the time of operation (E12.5). For example, the prospective joint-forming regions that are normally visualized by high levels of *HoxD* expression are not visible in digit rays III and IV 24 h after FGF4 exposure.

Our gene expression data, coupled with morphological analyses, disclosed a correlation between inhibition of growth and cartilage differentiation and prolonged expression of *Msx1* gene, along with altered expression patterns of *HoxD*s and *Igf2* genes in chondrogenic regions of digits III and IV. In addition, this analysis was able to highlight an asymmetry in gene expression patterns between chondrogenic tips III and IV in correlation with specific branching of digit IV. Indeed, presumptive bifurcations were correlated with an obvious widening of the *Igf2* gene expression area at the prechondrogenic tip IV, as well as a complementary widening of the *Msx1*-negative gene expression area at the same tip.

DISCUSSION

FGF4 Regulates Digit Morphogenesis

In the early limb bud, pattern formation is regulated in part by the activities of the AER and the ZPA in a feedback signaling loop that involves FGF4 expression by the AER (Laufer *et al.*, 1994; Niswander *et al.*, 1994). By the time the limb bud has reached digit-forming stages, both the AER and the ZPA have regressed (Wanek *et al.*, 1989; Wanek and Bryant, 1991). In this study, we have used ectopic application to study the action of FGF4 at a stage shortly after AER regression when endogenous levels of FGF4 are expected to be declining. This approach allows us to study how the spatial and temporal production of FGF4 influences cartilage patterning during the initiation of digit outgrowth. Our results indicate that ectopic FGF4 has two major effects on digit morphogenesis. First, it acts to inhibit chondrogenesis of the autopodial digit ray, and second, it acts in a position-specific manner on cells of the distal tip of digit IV to modify outgrowth and pattern formation. These results suggest that endogenous FGF4 plays a role in the initiation of distal outgrowth of digit skeletal elements.

Ectopic application of FGF4 into the mouse autopod results in a localized inhibition of chondrogenesis associated with proximal regions of the digit rudiment. A similar response has been reported in the chick limb (Buckland *et al.*, 1998; Merino *et al.*, 1998). Inhibition of chondrogenesis associated with FGF signaling also occurs in high-density cultures of anterior and posterior cells of the mouse limb bud (Anderson *et al.*, 1993, 1994). We show that the effect of FGF4 on chondrogenesis is not caused by an *in vivo* change in the rate of cell proliferation in proximal digit rudiments or by an increase in interdigital cell death. We do find localized changes in gene expression associated with the inhibition of chondrogenesis. FGF4 may alter cell fate by maintaining *Msx1* expression and retarding the progression

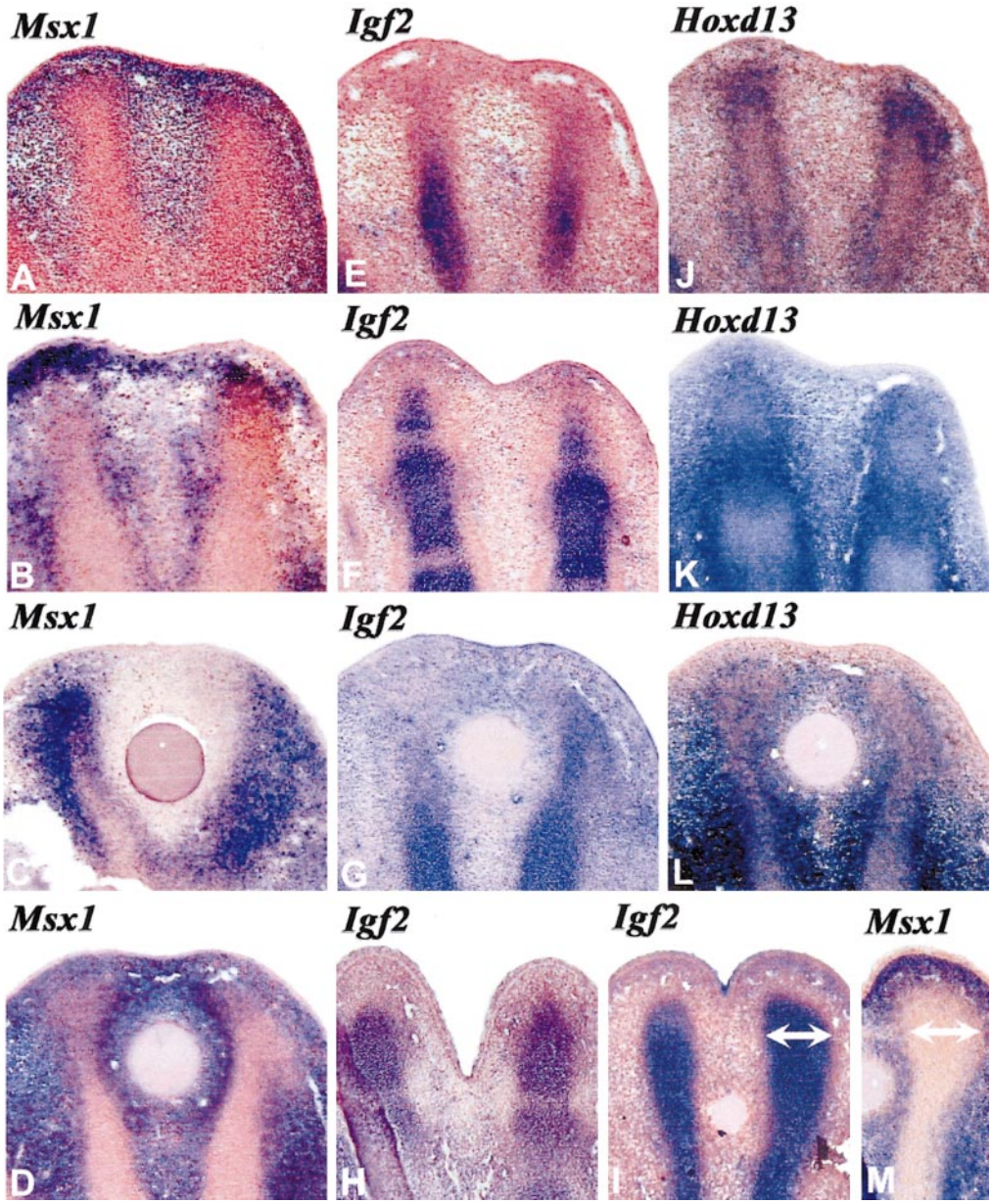

FIG. 4. FGF4 influences gene expression in E12.5 mouse hindlimb buds. Gene expression was analyzed by *in situ* hybridization on paraffin sections using DIG-labeled RNA probes. Specific mRNAs were revealed with BM purple staining, and sections were counterstained with safranin O. Ventral views of horizontal sections, with anterior to the left and distal toward the top. For clarity, only digit tips III and IV are illustrated, except for M (digit IV). Digit III is on the left and digit IV on the right of each photograph. (A, B, C, D, and M) *Msx1* expression pattern. (E, F, G, H, and I) *Igf2* expression pattern. (J, K, and L) *HoxD13* expression pattern. (A, E, and J) E12.5 control limbs. (B, F, and K) E13.5 control limbs. (C) E13.5 limb implanted with an FGF4 bead at early E12.5. (D, G, and L) E13.5 limbs implanted with an FGF4 bead at late E12.5. (H) E14.5 control limb. (I and M) E14.5 limbs implanted with an FGF4 bead at E12.5. Arrows denote widening of *Igf2* expression domain and *Msx1*-negative domain at the prechondrogenic tip of digit IV. Control limbs implanted with a control bead displayed the same expression patterns as unoperated control limbs, which were used for illustration.

of *Igf2* and posterior *HoxD* expression in chondrogenic regions. In this view, FGF4 may inhibit chondrogenesis by antagonizing BMP signaling associated with cartilage differentiation (Zou *et al.*, 1997). An antagonistic action of FGF and BMP signaling has been demonstrated in the early mouse limb bud (Niswander and Martin, 1993) and during digit formation in the chick limb bud (Buckland *et al.*, 1998).

Species-Dependent Plasticity of Interdigital Tissues

Our studies reveal both similarities and differences between chick and mouse digits with respect to the response to FGF4 application. As we discussed above there are clear similarities in the ways that FGF4 inhibits chondrogenesis in proximal digit rays both in the chick and in the mouse. The bifurcation response of prechondrogenic cells at the digit tip in the mouse appears to be distinct from that observed in the chick; however, as we address below, the observation that this response is restricted to digit IV complicates this interpretation and makes direct comparisons between species difficult. The most dramatic species-specific response to FGF4 involves the interdigital tissues of the mouse and the chick. In the chick, wounding of the interdigital region results in the formation of ectopic skeletal elements, whereas wounding the interdigital region of the mouse fails to elicit such a response. In addition, chick interdigital cells respond to FGF4 by inhibiting apoptosis resulting in an interdigital webbing phenotype, whereas in the mouse we observe a transient decline in apoptosis with no effect on digit separation. Finally, in the mouse *Msx1* gene expression is altered in prechondrogenic and chondrogenic regions in response to FGF4, whereas in the chick *Msx1* gene expression is unaffected by FGF4 (Macias *et al.,* 1996).

The tetrapod vertebrate limb anatomy is most divergent in the autopod and recent molecular evidence suggests that this diversity can be explained by modification of the *Hox* gene code (Tabin, 1992; Sordino *et al.,* 1995). Comparing the development of the autopod in birds and mammals, one striking difference centers on the utilization of interdigital tissues. In mammals there are few instances in which interdigital tissues participate in forming the adult limb pattern. In contrast, a large number of bird species (particularly waterfowl) retain interdigital tissue to form webbing that serves to increase the autopodial surface area, which is important for swimming. Such observations suggest that interdigital tissue must have come under differential selective pressure in the evolution of avian versus mammalian autopods and that as a result the interdigital tissues of birds and mammals have become differentially plastic in their response to extrinsic signals. Thus, avian interdigital tissues readily form ectopic skeletal elements in response to injury or TGFβ1 and form interdigital webbing in response to FGF4, whereas mammalian interdigital tissues do not respond in an analogous manner. Since mammalian interdigital tissues can undergo chondrogenesis *in vitro* and after ectopic transplantation (Lee *et al.,* 1993, 1994) and can form interdigital webbing (see Muragaki *et al.,* 1996; Zákány and Duboule, 1996; Witt and MacArthur, 1998), the data indicate that these cells have not lost this potential, only their level of plasticity.

FGF4 and Digit Bifurcation

In the mouse, we observe a distal bifurcation of the digit rudiment in response to FGF4, whereas in the chick no such response has been reported (Macias *et al.,* 1996; V. Ngo-Muller, unpublished results). Digit bifurcations are reported in the chick leg bud in experiments involving either control beads or beads releasing BMP that are placed directly at the apex of the digit (Gañan *et al.,* 1996). In these instances, bifurcations in the chick are thought to be caused either by mechanical factors (control bead or wounding) or by the induction of apoptosis to bisect the digit-forming region (BMP bead). In addition, recent work on *Pitx1* indicates that digit III bifurcation occurs in *Pitx1*-infected wings (Logan and Tabin, 1999). In this case, bifurcation is not mechanically induced, but results from the overexpression of the transcription factor in the whole wing bud. In our mouse FGF4 studies, the bifurcation is not mechanically induced because the bead is placed in the interdigital region, and we do not observe an ectopic region of cell death that might be responsible for the bifurcation. Thus, there appears to be evidence for species-specific differences in the way that the prechondrogenic region of the developing chick and mouse digit responds to FGF4.

Fate mapping the FGF4 response of the prechondrogenic digit tip indicates that the cells at the tip of the forming digit rudiment participate in digit bifurcation. Apoptosis of interdigital cells is transiently inhibited by FGF4; however, digit separation is not modified. This bifurcation response is therefore distinct from the phenomenon of ectopic digit formation from interdigital cells that has been well studied in the avian limb (Macias *et al.,* 1992, 1996; Ros *et al.,* 1994; Hurle and Colombatti, 1996). FGF4 does not modify the rate of cell proliferation in interdigital or prechondrogenic cells, indicating that the bifurcation response is not caused by a localized mitogenic signal. Previous *in vivo* fate maps of developing mouse digits (Muneoka *et al.,* 1989) along with our DiI labeling studies indicate that the proximal–distal level of digit bifurcation is caused by a reorganization of the prechondrogenic cells of the digit tip. This suggests that FGF4 acts as a chemoattractant, as demonstrated recently in chick early limb bud cells (Li and Muneoka, 1999). However, since FGF4 induces a similar reorganization of digit III prechondrogenic cells without inducing a bifurcation response, it seems unlikely that this chemotactic response is directly related to the bifurcation process.

Our data also indicate that FGF4 induces an increase in the size of prechondrogenic and chondrogenic domains at the digit tip, as evidenced by the enlargement of the *Igf2* and *Msx1* expression domains. The enlargement of the prechondrogenic domain may be a prerequisite for a bifurcation response, i.e., the prechondrogenic region would have to reach a critical mass for bifurcation to occur. We note that an expansion of a cartilage-condensing domain can induce a mathematical bifurcation in mechanochemical models of skeletal pattern formation (see Oster and Murray, 1989).

One way to explain how bifurcation occurs is to hypothesize that FGF4 induces the duplication of a putative signaling center, which instructs prechondrogenic condensations to grow distally, and that digit IV bifurcation results from outgrowth with reference to the resulting two distinct

boundaries. The hypothesis that digit formation is controlled by an FGF4-sensitive distal boundary is strengthened by the observation that the bifurcations are always perfectly symmetrical (Fig. 1C). Since we see no difference in mesenchymal cell behavior in response to FGF4 between the nonbifurcating cells of digit III and the bifurcating cells of digit IV, we believe that this distal signal is produced by the ectoderm. The lack of a bifurcation response in digit III is associated with an FGF4-induced cell migration response, thus we conclude that the distal ectoderm of digit III is FGF4-insensitive.

Thus we propose a model in which FGF4 would serve a dual role during skeletal branching of digit IV. First, FGF4 would have a direct chemotactic effect on mesenchymal cells, resulting in an increase in the physical size of the prechondrogenic domain. Second, FGF4 would play a role in establishing an ectodermal signaling center responsible for directing distal outgrowth of prechondrogenic cells. The dual effect of FGF4 is required for the observed digit IV bifurcation response. According to this model, the alterations of gene expression observed in response to FGF4 may reflect cell fate modification (including chondrogenic inhibition and spatial rearrangement), rather than being instrumental in the bifurcation process.

FGF4 and the Evolution of Vertebrate Limb Patterning

In our studies, the absence of an FGF4-induced distal bifurcation response in digits II or III is significant and suggests a characteristic unique to digit IV. One aspect unique to digit IV in the mouse is that it is the first autopodial condensation to appear, followed in sequence by digits III, II, V, and I (see Wanek *et al.*, 1989). A simple explanation would be that this FGF4 bifurcation response is stage-specific; however, we have tested this hypothesis and do not observe an FGF4-induced bifurcation response in other digits at later stages. The unique propensity of digit IV to undergo a branching event is consistent with the idea that branching events that are important for limb patterning are spatially restricted during development. Shubin and Alberch (1986) have proposed that the vertebrate limb skeletal pattern forms through a hierarchical sequence of chondrogenic branching and segmentation events. The evolution of the diverse morphologies of the vertebrate limb is thought to result from spatial–temporal changes in the pattern of these branching and segmentation events. The hypothetical axis from which branching events arise is called the metapterygial axis and the identification of this primitive axis has remained a mystery. It is generally viewed that the metapterygial axis runs along the proximal–distal axis on the posterior side of the limb in the proximal region. However, the distal placement of this primitive axis has been variously hypothesized to run through any of the digits, between digits, or curving from posterior to anterior in congruence with the digital arch (reviewed by Shubin and Alberch, 1986). The evidence supporting one hypothesized metapterygial axis over another is largely based on comparative limb morphologies rather than on direct experimentation. One way to interpret digit IV-specific bifurcation is to consider our data with respect to this view of sequential bifurcations of the metapterygial axis. We propose that the metapterygial axis can be experimentally defined based on its propensity toward chondrogenic branching events and that our bifurcation data indicate that digit IV represents the distal path of this axis in the mouse. Anatomical data placing the distal portion of the metapterygial axis in digit IV has been previously reported (see Watson, 1913). Our model for digit bifurcation also supports the idea that the metapterygial axis is defined by the properties of the ectoderm rather than the mesenchyme. An important implication of this model is that it places FGF4 signaling in a key position to direct skeletal branching during limb morphogenesis and, as such, playing a defining role in the evolution of vertebrate digit diversity.

ACKNOWLEDGMENTS

We thank Scott S. Schaller for technical help and Rosalie A. Anderson and Minoru Omi for comments on the manuscript. V.N.-M. was supported by a fellowship from the Association pour la Recherche contre le Cancer. This work was supported by HD35245.

REFERENCES

Anderson, R., Landry, M., and Muneoka, K. (1993). Maintenance of ZPA signaling in cultured mouse limb bud cells. *Development* **117,** 1421–1433.

Anderson, R., Landry, M., Reginelli, A., Taylor, G., Achkar, C., Gudas, L., and Muneoka, K. (1994). Conversion of anterior limb bud cells to ZPA signaling cells *in vitro* and *in vivo*. *Dev. Biol.* **164,** 241–257.

Bell, J. R., Noveen, A., Liu, Y. H., Ma, L., Dobias, S., Kundu, R., Luo, W., Xia, Y., Lusis, A. J., Snead, M. L., *et al.* (1993). Genomic structure, chromosomal location, and evolution of the mouse Hox 8 gene. *Genomics* **17,** 800.

Brown, J. M., Wedden, S. E., Millburn, G. H., Robson, L. G., Hill, R. E., Davidson, D. R., and Tickle, C. (1993). Experimental analysis of the control of expression of the homeobox-gene Msx-1 in the developing limb and face. *Development* **119,** 41–48.

Bryant, S. V., and Iten, L. (1974). The regulative ability of the limb regeneration blastema of Notophthalmus viridescens: Experiments *in situ*. *Wilhelm Roux Arch.* **174,** 90–101.

Buckland, R. A., Collinson, J. M., Graham, E., Davidson, D. R., and Hill, R. E. (1998). Antagonistic effects of FGF4 on BMP induction of apoptosis and chondrogenesis in the chick limb bud. *Mech. Dev.* **71,** 143–150.

Chen, Y., and Zhao, X. (1998). Shaping limbs by apoptosis. *J. Exp. Zool.* **282,** 691–702.

Crossley, P. H., Minowada, G., MacArthur, C. A., and Martin, G. R. (1996). Roles for FGF8 in the induction, initiation, and maintenance of chick limb development. *Cell* **84,** 127–136.

Dollé, P., Izpisua-Belmonte, J-C., Falkenstein, H., Renucci, A., and Duboule, D. (1989). Coordinate expression of the murine Hox-5

complex homeobox-containing genes during limb pattern formation. *Nature* **342,** 767–772.

Fallon, J. F., Lopez, A., Ros, M. A., Savage, M. P., Olwin, B. B., and Simandl, B. K. (1994). FGF-2: Apical ectodermal ridge growth signal for chick limb development. *Science* **264,** 104–107.

Gañan, Y., Macias, D., Duterque-Coquillaud, M., Ros, M. A., and Hurle, J. M. (1996). Role of TGF betas and BMPs as signals controlling the position of the digits and the areas of interdigital cell death in the developing chick limb autopod. *Development* **122,** 2349–2357.

Ghosh, A. K., Shankar, D. B., Shackleford, G. M., Wu, K., T'Ang, A., Miller, G. J., Zheng, J., and Roy-Burman, P. (1996). Molecular cloning and characterization of human FGF8 alternative messenger RNA forms. *Cell Growth Differ.* **7,** 1425–1434.

Goff, D. J., and Tabin, C. J. (1997). Analysis of Hoxd-13 and Hoxd-11 misexpression in chick limb buds reveals that Hox genes affect both bone condensation and growth. *Development* **124,** 627–636.

Hamburger, V., and Hamilton, H. L. (1951). A series of normal stages in the development of the chick embryo. *J. Morphol.* **88,** 49–92.

Hinchliffe, J. R., and Horder, T. J. (1993). Lessons from extra-digits. *In* "Limb Development and Regeneration" (J. F. Fallon *et al.*, Eds.), pp. 113–126. Wiley–Liss, New York.

Humason, G. L. (1972). "Animal Tissue Techniques" (D. Kennedy and R. B. Park, Eds.). Freeman, San Francisco.

Hurle, J. M., Gañan, Y., and Macias, D. (1989). Experimental analysis of the *in vivo* chondrogenic potential of the interdigital mesenchyme of the chick leg bud subjected to local ectodermal removal. *Dev. Biol.* **132,** 368–374.

Hurle, J. M., and Colombatti, A. (1996). Extracellular matrix modifications in the interdigital spaces of the chick embryo leg bud during the formation of ectopic digits. *Anat. Embryol.* **193,** 355–364.

Itoh, N., Mima, T., and Mikawa, T. (1996). Loss of fibroblast growth factor receptors is necessary for terminal differentiation of embryonic limb muscle. *Development* **122,** 291–300.

Johnson, R. L., and Tabin, C. J. (1997). Molecular models for vertebrate limb development. *Cell* **90,** 979–990.

Kostakopoulou, K., Vargesson, N., Clarke, J. D., Brickell, P. M., and Tickle, C. (1997). Local origin of cells in FGF4—Induced outgrowth of amputated chick wing bud stumps. *Int. J. Dev. Biol.* **41,** 747–750.

Laufer, E., Nelson, C. E., Johnson, R. L., Morgan, B. A., and Tabin, C. (1994). Sonic hedgehog and FGF4 act through a signaling cascade and feedback loop to integrate growth and patterning of the developing limb bud. *Cell* **79,** 993–1003.

Lee, K. K., Chan, W. Y., and Sze, L. Y. (1993). Histogenetic potential of rat hind-limb interdigital tissues prior to and during the onset of programmed cell death. *Anat. Rec.* **236,** 568–572.

Lee, K. K., Li, F. C., Yung, W. T., Kung, J. L., Ng, J. L., and Cheah, K. S. (1994). Influence of digits, ectoderm, and retinoic acid on chondrogenesis by mouse interdigital mesoderm in culture. *Dev. Dyn.* **201,** 297–309.

Li, S., Anderson, R., Reginelli, A. D., and Muneoka, K. (1996). FGF-2 influences cell movements and gene expression during limb development. *J. Exp. Zool.* **274,** 234–247.

Li, S., and Muneoka, K. (1999). Cell migration and chick limb development: Chemotactic action of FGF4 and the AER. *Dev. Biol.* **211,** 335–347.

Logan, M., and Tabin, C. J. (1999). Role of pitx1 upstream of tbx4 in specification of hindlimb identity. *Science* **283,** 1736–1739.

Maconnachie, E. (1979). A study of digit fusion in the mouse embryo. *J. Embryol. Exp. Morphol.* **49,** 259–276.

Macias, D., Gañan, Y., and Hurle, J. M. (1992). Interdigital chondrogenesis and extra digit formation in the duck leg bud subjected to local ectoderm removal. *Anat. Embryol.* **186,** 27–32.

Macias, D., Gañan, Y., Ros, M. A., and Hurle, J. M. (1996). *In vivo* inhibition of programmed cell death by local administration of FGF-2 and FGF4 in the interdigital areas of the embryonic chick leg bud. *Anat. Embryol.* **193,** 533–541.

Merino, R., Gañan, Y., Macias, D., Economides, A. N., Sampath, K. T., and Hurle, J. M. (1998). Morphogenesis of digits in the avian limb is controlled by FGFs, TGFβs, and noggin through BMP signaling. *Dev. Biol.* **200,** 35–45.

Muneoka, K., Wanek, N., and Bryant, S. V. (1989). Mammalian limb bud development: *In situ* fate maps of early hindlimb buds. *J. Exp. Zool.* **249,** 50–54.

Muragaki, Y., Mundlos, S., Upton, J., and Olsen, B. R. (1996). Altered growth and branching patterns in synpolydactyly caused by mutations in HOXD13. *Science* **272,** 548–551.

Niswander, L., and Martin, G. R. (1992). FGF4 expression during gastrulation, myogenesis, limb and tooth development in the mouse. *Development* **114,** 755–768.

Niswander, L., and Martin, G. R. (1993). FGF4 and BMP-2 have opposite effects on limb growth. *Nature* **361,** 68–71.

Niswander, L., Tickle, C., Vogel, A., Booth, I., and Martin, G. R. (1993). FGF4 replaces the apical ectodermal ridge and directs outgrowth and patterning of the limb. *Cell* **75,** 579–587.

Niswander, L., Jeffrey, S., Martin, G. R., and Tickle, C. (1994). A positive feedback loop coordinates growth and patterning in the vertebrate limb. *Nature* **371,** 609–612.

Ngo-Muller, V., and Muneoka, K. (1999). Exo utero surgery. *In* "Methods in Molecular Biology, Vol. 135, Developmental Biology Protocols, Vol. I" (R. S. Tuan and C. W. Lo, Eds.). Humana Press, Totowa, NJ. pp. 481–492.

Oster, G. F., and Murray, J. D. (1989). Pattern formation models and developmental constraints. *J. Exp. Zool.* **251,** 186–202.

Reginelli, A. D., Wang, Y. Q., Sassoon, D., and Muneoka, K. (1995). Digit tip regeneration correlates with regions of Msx1 (Hox 7) expression in fetal and newborn mice. *Development* **121,** 1065–1076.

Rijli, F. M., and Chambon, P. (1997). Genetic interactions of Hox genes in limb development: Learning from compound mutants. *Curr. Opin. Genet. Dev.* **7,** 481–487.

Ros, M. A., Macias, D., Fallon, J. F., and Hurle, J. M. (1994). Formation of extra digits in the interdigital spaces of the chick leg bud is not preceded by changes in the expression of the Msx and Hoxd genes. *Anat. Embryol.* **190,** 375–382.

Savage, M. P., Hart, C. E., Riley, B. B., Sasse, J., Olwin, B. B., and Fallon, J. F. (1993). Distribution of FGF-2 suggests it has a role in chick limb bud growth. *Dev. Dyn.* **198,** 159–170.

Shubin, H., and Alberch, P. (1986). A morphogenetic approach to the origin and basic organization of the tetrapod limb. *Evol. Biol.* **20,** 319–387.

Sordino, P., van der Hoeven, F., and Duboule, D. (1995). Hox gene expression in teleost fins and the origin of vertebrate digits. *Nature* **375,** 678–681.

Summerbell, D., Lewis, J. H., and Wolpert, L. (1973). Positional information in chick limb morphogenesis. *Nature* **244,** 492–496.

Tabin, C. J. (1992). Why we have (only) five fingers per hand: Hox genes and the evolution of paired limbs. *Development* **116,** 289–296.

van Kleffens, M., Groffen, C., Rosato, R. R., van den Eijnde, S. M., van Neck, J. W., Lindenbergh-Kortleve, D. J., Zwarthoff, E. C., and Drop, S. L. (1998). mRNA expression patterns of the IGF system during mouse limb bud development, determined by whole mount *in situ* hybridization. *Mol. Cell. Endocrinol.* **138,** 151–161.

Vihinen, T., Auvinen, P., Alanen-Kurki, L., and Jalkanen, M. (1993). Structural organization and genomic sequence of mouse syndecan-1 gene. *J. Biol. Chem*. **268,** 17261–17269.

Vogel, A., Rodriguez, C., and Izpisua-Belmonte, J-C. (1996). Involvement of FGF-8 in initiation, outgrowth and patterning of the vertebrate limb. *Development* **122,** 1737–1750.

Walterhouse, D., Ahmed, M., Slusarski, D., Kalamaras, J., Boucher, D., Holmgren, R., and Iannaccone, P. (1993). *gli*, a zinc finger transcription factor and oncogene, is expressed during normal mouse development. *Dev. Dyn.* **196,** 91–102.

Wanek, N., Muneoka, K., Holler-Dinsmore, G., Burton, R., and Bryant, S. V. (1989). A staging system for mouse limb development. *J. Exp. Zool.* **249,** 41–49.

Wanek, N., and Bryant, S. V. (1991). Temporal pattern of posterior positional identity in mouse limb buds. *Dev. Biol.* **147,** 480–484.

Watson, D. M. S. (1913). On the primitive tetrapod limb. *Anat. Anz.* **44,** 24–27.

Webb, S. E., Lee, K. K., Tang, M. K., and Ede, D. A. (1997). Fibroblast growth factors 2 and 4 stimulate migration of mouse embryonic limb myogenic cells. *Dev. Dyn.* **209,** 206–216.

Wilkinson, D. G., and Nieto, M. A. (1993). Detection of messenger RNA by *in situ* hybridization to tissue sections and whole mounts. *In* "Methods in Enzymology," Vol. 255, pp. 361–372. Academic Press, San Diego.

Witt, P. D., and MacArthur, C. A. (1998). Molecular biology and congenital hand anomalies: From molecules and mutations to man. *Plast. Reconstr. Surg.* **102,** 2254–2267.

Yokouchi, Y., Sasaki, H., and Kuroiwa, A. (1991). Homeobox gene expression correlated with the bifurcation process of limb cartilage development. *Nature* **353,** 443–445.

Yokouchi, Y., Nakazato, S., Yamamoto, M., Goto, Y., Kameda, T., Iba, H., and Kuroiwa, A. (1995). Misexpression of Hoxa-13 induces cartilage homeotic transformation and changes cell adhesiveness in chick limb buds. *Genes Dev.* **9,** 2509–2522.

Yokouchi, Y., Sakiyama, J., Kameda, T., Iba, H., Suzuki, A., Ueno, N., and Kuroiwa, A. (1996). BMP-2/-4 mediate programmed cell death in chicken limb buds. *Development* **122,** 3725–3734.

Zákány, J., and Duboule, D. (1996). Synpolydactyly in mice with a targeted deficiency in the HoxD complex. *Nature* **384,** 69–71.

Zou, H., and Niswander, L. (1996). Requirement for BMP signaling in interdigital apoptosis and scale formation. *Science* **272,** 738–741.

Zou, H., Wieser, R., Massague, J., and Niswander, L. (1997). Distinct roles of type I bone morphogenetic protein receptors in the formation and differentiation of cartilage. *Genes Dev.* **11,** 2191–2203.

Received for publication July 13, 1999
Revised November 10, 1999
Accepted December 28, 1999